NASA Contractor Report 195352

Slow Wave Vane Structure With Elliptical Cross-Section Slots, an Analysis

Henry G. Kosmahl
Analex Corporation
Brook Park, Ohio

November 1994

Prepared for
Lewis Research Center
Under Contract NAS3–25776

National Aeronautics and
Space Administration

TABLE OF CONTENTS

SLOW WAVE VANE STRUCTURE WITH ELLIPTICAL CROSS-SECTION SLOTS, AN ANALYSIS

Henry G. Kosmahl, Fellow IEEE[1]
Analex Corporation
3001 Aerospace Parkway
Brook Park, Ohio 44142

Abstract—Mathematical analysis of the wave equation in cylinders with elliptical cross-section slots was performed. Compared to slow wave structures with rectangular slots higher impedance and lower power dissipation losses are evident below a certain value of *kh*. These features could lead to improved designs of traveling wave magnetrons and gigahertz backward-wave oscillators as well as linear traveling wave tubes with relatively shallow slots.

INTRODUCTION

The slow wave, slotted vane structure with or without an opposite parallel plane (Fig. 1) has been studied in numerous studies (e.g., by Watkins [2] and by Collins [4]) in more depth. In either a linear version, as in Fig. 1, or in circularly bent configuration this structure has been successfully used as slow wave circuit in traveling wave crossed field amplifiers or oscillators. The structure has a forward wave fundamental with a backward wave as first space harmonic. The latter has served as the most successful circuit for very high frequency: 300 to 2000 GHz, milliwatt power (backward wave) voltage tunable oscillator. On the positive side, the favorable feature of this structure is its very high beam interaction impedance, when the beam hole is placed into the vane just below $y = 0$. There the electric field decreases slowly as $\sin k(y - y_o)$ and $\sin ky_o \approx 0$, y_o being the center of the beam hole. For this reason the transverse beam—slow wave structure—coupling coefficient is very large, $M_2 \geq 0.9$, much larger than in helices, coupled cavities, and similar structures with exponential decay. On the negative side, this low pass filter circuit has a typical $kh = \omega h/c$ versus $\beta_o L$ characteristic: the curve rises rapidly with high velocity $u_{ph} \approx c/2$ to a point where $\beta_o L$ is approximately $\pi/3$, bends over into an almost horizontal (parallel to $\beta_o L$) shape where the group velocity u_g is a small fraction of c, $u_g \approx c/100$. One is thus forced to work inside the "bend" region and compromise between high beam coupling impedance $K \propto 1/u_g$ and losses, also proportional to $1/u_g$. With rectangular slots it is not too difficult to achieve $K \approx 200$ to 300 Ω with acceptable losses on a short circuit. High impedance makes this circuit also attractive for low power, low voltage applications at 30 GHz, providing that construction of a circuit with vane spacing equal to approximately 1/5 mm ≈ 200 μm is successful! If it is, electrostatic beam focusing with a converging-diverging beam without external fields is feasible.

[1]Work performed for and supported by the Electron Beam Technology Branch, NASA Lewis Research Center, Cleveland, Ohio.

The analysis described by Collins in [4] does not assume a constant electric field in the gap at $y = 0$. By expanding the electric and magnetic fields across the gap of the form

$$E_z(z, y = 0)e^{i\omega t} = \sum_{n=-\infty}^{\infty} E_n \, e^{-i\beta_n Z} e^{i\omega t}$$

inside the gap $0 < z < \delta$; $E_z = 0$, $\delta < z < L$; an infinite by infinite determinant is obtained whose zero value yield the coefficients E_n; analysis performed† shows that the zero coefficient E_{no} (as assumed by Watkins [2]) alone gives an accuracy of more that 98 percent, that is $E_z \cong$ constant to within 1 to 2 percent across the gap!

In this study the replacement of the rectangular slot by one with an elliptical cross section with the small semi-axis = $\delta/2$ and the large = h has been examined with full rigor, except for assuming the constancy of E_z across the gap as discussed earlier. Results confirm expected behavior: due to smaller volume and shorter boundaries the slot energy and the power dissipation in elliptical slots are smaller than those in rectangular slots. That means doubling the impedance and cutting the losses, a very attractive feature for potential applications. Fabrication experiments have shown that elliptical slots are not feasible to construct with an aspect ratio $h/\delta = 15$, as required by low voltage requirement $V_o \leq 6$ kV for a 2 W, 30 GHz forward wave TWT. On the other side, higher voltage, low frequency crossed field amplifiers could much benefit from higher impedance and lower losses. Since noise jitter and noise figure are proportional to the current (at least in the first power), efficiency and noise could be improved.

The vane structure with elliptical slots could be used for design and construction of a BWO with lower starting oscillation current due to higher K and lower losses.

In the analysis to follow the wave equation of an elliptic cylinder is solved, assuming a single component for E_z that behaves like the elliptic sine, in analogy to the treatment by Watkins. Although rigorous expressions were derived, it would require extensive programming of Mathieu functions to established rigorous results. Such a project should, perhaps, be carried out if interest in the possible applications is demonstrated.

LIST OF SYMBOLS

A_r^1	coefficients of expansion in Mathieu functions
a_m, b_m	characteristic numbers in Mathieu equations
C	constants

† Unpublished work at LeRC.

c	speed of light = $(\varepsilon_o \mu_o)^{-1/2}$
c_o	half confocal length of ellipses
$C_{em}(\xi,q)$, $Se_m(\xi,q)$, $Fey_m(\xi,q)$, $Gey_m(\xi,q)$	Radial Mathieu Function
$ce_m(\eta,q)$, $se_m(\eta,q)$	"elliptic cosine" and "elliptic sine" Mathieu Functions
d	distance between top of vanes and opposite planar conductor
E	electric field, [*V/cm*]
f	frequency
$f(q, kh)$	function, Eq. (33)
$g = \left(c_o/\sqrt{2}\right)\sqrt{\cosh 2\xi - \cos 2\eta}$	metric factor in elliptical coordinates
H	magnetic field, [*A/cm*]
h	height of vanes
K	interaction impedance [Ω]
$k = \omega/c$	wave number in vacuum
L	period in slow wave structures
M	longitudinal or transverse beam-wave coupling coefficient
m	order of elliptic functions ce_m, Ce_m, etc., interger
m	number of slot in periodic structure, interger
P	power [watts]
$q = k^2 c_o^2/4$	parameter in Mathieu equations
$R'_{[]}$	Skin effect surface resistivity [Ω]
u_{ph}, u_g	phase or group velocity, [cm/sec]
W	stored energy, [Joule]
w	width
x, y, z	carthesian coordinates
Z_o	$\sqrt{\mu_o/\varepsilon_o}$ wave impedance in vacuum [Ω]
Z_n	ordinary Bessel Functions J_n or N_n

GREEK SYMBOLS

$\alpha_3, \alpha_5 \ldots$	coefficients, Eq. (13)
β_n	slow wave propagation constant, axial
$\gamma_n = +\sqrt{\beta_n^2 - k^2}$	slow wave propagation constant, radial

δ	clear space between vanes
ξ,η,x	coordinates of an elliptical cylinder
ε_o	permittivity of free space
$\zeta(\xi,\eta) = \Psi(\xi) \cdot \phi(\eta)$	product solution of wave equation in elliptical slots
λ_o	free space wavelength [cm]
μ_o	permeability of free space

SUBSCRIPTS

D	discipitated
m	number of slot, interger
m	order of elliptic (Mathieu) functions
n	summation index for slow waves
e	refers to elliptic
r	order of coefficients, A_r, interger

WAVE EQUATION IN ELLIPTICAL COORDINATES

In solving the wave equation inside the slots of elliptical cross section we are dealing with the geometry of an elliptical cylinder that extends infinitely in the x-direction $(\partial/\partial x = 0)$. When the two-dimensional wave equation in vacuum

$$\frac{\partial^2 \begin{Bmatrix} E \\ H \end{Bmatrix}}{\partial y^2} + \frac{\partial^2 \begin{Bmatrix} E \\ H \end{Bmatrix}}{\partial z^2} + k^2 \begin{Bmatrix} E \\ H \end{Bmatrix} = 0; \quad k = \frac{\omega}{c} = \omega\sqrt{\mu_o \varepsilon_o} \tag{1}$$

is transformed from the cartesian coordinates x,y,z into confocal elliptical coordinates [1], one obtains, see Fig 2,

$$\frac{\partial^2 \varsigma}{\partial \xi^2} + \frac{\partial^2 \varsigma}{\partial \eta^2} + \frac{2k^2 c_o^2}{4} (\cosh 2\xi - \cos 2\eta)\, \varsigma = 0 \tag{2}$$

where $\zeta(\xi,\eta) = \psi(\xi)\cdot\phi(\eta)$ and Ψ is a function of ξ alone and ϕ a function of η alone. Then we obtain

$$\phi \frac{\partial^2 \psi}{\partial \xi^2} + \psi \frac{\partial^2 \phi}{\partial \eta^2} + \frac{2k^2 c_o^2}{4} (\cosh 2\xi - \cos 2\eta)\psi \cdot \phi = 0 \tag{3}$$

and $\varsigma = \psi \cdot \phi$ is either E or H.

Dividing Eq. (3) by $\psi \cdot \phi$ leads to:

$$\frac{1}{\psi}\frac{d^2\psi}{\partial\xi^2} + \frac{2k^2c_o^2}{4}\cosh 2\xi = -\frac{1}{\phi}\frac{d^2\phi}{\partial\eta^2} + \frac{2k^2c_o^2}{4}\cos 2\eta = a \tag{4}$$

where a is a separation constant. Rearranging leads to two ordinary equations:

$$\frac{d^2\phi}{\partial\eta^2} + \left(a - \frac{2k^2c_o^2}{4}\cos 2\eta\right)\phi = 0 \tag{5}$$

$$\frac{d^2\psi}{\partial\xi^2} - \left(a - \frac{2k^2c_o^2}{4}\cosh 2\xi\right)\psi = 0 \tag{6}$$

Equations (5) and (6) are called the canonical forms of Mathieu equations. If in Eq. (5) we write $\pm i\xi$ for η, it is transformed into Eq. (6), while (6) is transformed into Eq. (5) if $\pm i\eta$ is used for ξ. Sometimes this is considered a fluke—but a lucky and useful one. Two functions which are solutions of Eqs. (5) and (6), respectively, for the same values of a and $q = k^2 c_o^2/4$ form a product that yields the desired functions $\varsigma = \psi \cdot \phi = H$ or E. Since a may have any value, the number of solutions could become unrestricted. However, the electromagnetic field is a periodic and single valued function of η and ξ and its solutions are linear functions. This is possible only for discrete values of the separation constants a, called "characteristic numbers" $a = a_m, b_m$. They yield, in turn, ordinary and modified Mathieu functions of integer order m, corresponding to a_m, b_m. Observe that we are interested only in cases where $q = k^2c_o^2/4$ is positive, $q > 0$.

The periodic solutions of Eq. (5) of first kind are denoted either $ce_m(\eta, q)$ or $se_m(\eta, q)$—an abbreviation of "cosine-elliptic" or "sine-elliptic"—are the ordinary Mathieu functions, while the "Radial" solutions $Ce_m(\xi, q)$ and $Se_m(\xi, q)$ and $Fey_m(\xi, q)$ are called modified Mathieu functions of the order m. They have to be combined to form the product solutions that belong to the separation constants a_m,

$$Ce_m(\xi, q)ce_m(\eta, q),\ Fey_m(\xi, q)ce_m(\eta, q) \tag{7}$$

and

$$Se_m(\xi, q)se_m(\eta, q),\ Gey_m(\xi, q)se_m(\eta, q) \tag{8}$$

that belong to the separation constant b_m.

The corresponding functions in cases of circular cylinders (e.g., helix) are the ordinary or modified Bessel functions (e.g., $I_m(\gamma_m\tau)K(\gamma_m\tau)$ or $J_m(\gamma_m\tau)N(\gamma_m\tau)$ and $\cos(m\eta)$ or $\sin(m\eta)$. Notice that, in general, $a_m \neq b_m$ and that mixing of Mathieu functions other than that shown in (7) and (8) is not permitted. The power series for ordinary and modified Mathieu functions were computed and tabulations may be found in [1] and [3].

DISPERSION EQUATION

We shall derive in this paragraph the dispersion relation $\beta(\omega) = f(\omega/c) = f(k)$ for the finned structure shown in Fig. 1 with slots having an elliptical shape. Since it is assumed that the slots extend infinitely in the x-direction (perpendicular to the plane of paper) we are dealing with elliptical cylinders with no x variation, $\partial/\partial x = 0$; it is very helpful and necessary to invoke the comparison with the case of rectangular slots, as treated by Watkins [2]. Watkins takes only the O-order case with no variation of E and H along the boundary $y = 0$. The appropriate solution for standing waves in cartesian coordinates is then [2] in the m-th slot (not to be confused with order in above)

$$E_z = E_o \frac{\sin k(y+h)}{\sin kh} e^{-i\beta_o mL} \quad mL < z < mL + \delta \tag{9}$$

$$E_z = O, mL + \delta < z < (m+1)L \tag{9a}$$

$$i\omega\mu_o H_x = -\text{curl } E_z; H_x = \text{i}\sqrt{\frac{\varepsilon_o}{\mu_o}} \frac{\cos k(y+h)}{\sin kh} \text{e}^{-i\beta_o mL} \tag{10}$$

$$H_x = 0,\ mL + \delta < z\ (m+1)\,L \tag{10a}$$

$$E_x = E_y = H_y = H_z \equiv 0 \tag{11}$$

We take notice that both E and H are independent of z inside the rectangular slots! We are dealing with a TEM wave only. Returning now to the case to be treated in elliptical cylinder coordinates it seems appropriate to use the Ansatz yielding results of the form of Eqs. (9) and (10). Since H_x is in the direction of the axis of the elliptic cylinder that has a maximum at the apex (bottom of slot), $\eta = 0$, we put the linear combination

$$H_x(\eta,\xi) = C\,ce_1(\eta,q)\cdot\left[Ce_1(\xi,q) + \frac{C_2}{C_1}\ Fey_1(\xi,q)\right] \tag{12}$$

Equation (12) is the (product) solution of wave Eq. (2) in elliptic cylinder coordinates. Note that $H_x(\eta,\xi)$ is independent of x. $ce_1(\eta,q)$, $Ce_1(\xi,q)$and Fey_1 are the angular and radial solutions of Eqs. (5) and (6), respectively and are given in [1] and [3].

$$ce_1(\eta,q) = \cos\eta - \underbrace{\frac{q}{8}\left(1+\frac{q}{8}+\frac{q^2}{192}+-\cdots\right)}_{\alpha_3}\cos 3\eta + \underbrace{\frac{q^2}{192}\left(1+\frac{q}{6}+\cdots\right)}_{\alpha_5}\cos 5\eta - + \cdots \tag{13}$$

For values of q not too large ($q<8$), the series converges quickly. In our case $q \le \pi^2/16 \le 0.61685$. The radial functions are

$$Ce_1(\xi,q) = \frac{ce_1'\left(\frac{\pi}{2},q\right)}{\sqrt{q}A_1^1}\left[-A_1^1 J_1\left(2\sqrt{q}\cosh\xi\right) + A_3^1 J_3\left(2\sqrt{q}\cosh\xi\right) - A_5^1 J_5\left(2\sqrt{q}\cosh\xi\right) + - \quad\right] \tag{14a}$$

$$Fey_1(\xi,q) = \frac{ce_1'\left(\frac{\pi}{2},q\right)}{\sqrt{qA_1^1}}\left[-A_1^1 N_1\left(2\sqrt{q}\cosh\xi\right) + A_3^1 N_3\left(2\sqrt{q}\cosh\xi\right) - A_5^1 N_5\left(2\sqrt{q}\cosh\xi\right) + - \cdots\right] \tag{14b}$$

In Eq. (14)

$$ce_1'\left(\frac{\pi}{2},q\right) = \left.\frac{\partial ce_1(\eta,q)}{\partial\eta}\right|_{\eta=\pi/2} = -\left[1+\frac{3}{8}q\left(1+\frac{q}{8}+\frac{q^2}{192}\right)+\frac{5}{192}q^2\left(1+\frac{q}{6}+\quad\right)+-\ldots\right] \tag{13a}$$

After dividing Eq. (14) by A_1^1, Eqs. (14) may be written

$$Ce_1(\xi,q) = -\frac{ce_1'\left(\frac{\pi}{2},q\right)}{\sqrt{q}}\left[J_1\left(2\sqrt{q}\cosh\xi\right) - \frac{A_3^1}{A_1^1}J_3\left(2\sqrt{q}\cosh\xi\right) + \frac{A_5^1}{A_1^1}J_5\left(2\sqrt{q}\cosh\xi\right) - \cdots\right] \tag{14a}$$

$$Fey_1(\xi,q) = -\frac{ce_1'\left(\frac{\pi}{2},q\right)}{\sqrt{q}}\left[N_1\left(2\sqrt{q}\cosh\xi\right) - \frac{A_3^1}{A_1^1}N_3\left(2\sqrt{q}\cosh\xi\right) + -\ldots\right] \tag{14b}$$

For an ellipse whose long half axis $a = c_o\cosh\xi >> b = c_o\sinh\xi = \frac{\delta}{2}$ = half gap width.

$$c_o = \sqrt{a^2-b^2} = \sqrt{h^2-\frac{\delta^2}{4}},\ \cosh\xi = \frac{a}{c_o} = \frac{h}{\sqrt{h^2-\frac{\delta^2}{4}}} = \frac{h}{h\sqrt{1-\frac{\delta^2}{4h^2}}} \approx 1+\frac{1}{8}\frac{\delta^2}{h^2}$$

With $\frac{\delta}{h} = \frac{1}{15}$ as required for a 30 GHz TWT, $\cosh\xi_o = 1.000556$; and $\xi_o = 0.03345$,

with a small error cosh ξ can be taken as 1 in the arguments of the Bessel functions. Thus:

$$Ce_1(\xi,q) = -\frac{ce_1'\left(\frac{\pi}{2},q\right)}{\sqrt{q}}\left[J_1(kc_o) - \frac{A_3^1}{A_1^1}J_3(kc_o) + \frac{A_5^1}{A_1^1}J_5(kc_o) - \cdots\right] \tag{14c}$$

And because $\delta << h$, $c_o \approx h$, and Eq. (14b) may be changed to

$$Ce_1(\xi,q) \approx -\frac{ce_1'\left(\frac{\pi}{2},q\right)}{\sqrt{q}}\left[J_1(kh) - \frac{A_3^1}{A_1^1}, J_3(kh) + \frac{A_5^1}{A_1^1}, J_5(kh)\right] \tag{14d}$$

and similar for the Fey_1 function.

Expressions for the coefficients A'_{2n+1} will be derived later. On the long axis $\xi = 0$, on the ellipse $\xi = \xi_o$ and the argument of the Bessel series, kh, changes to $1.00055\,kh$ with negligible change in the Ce and Fey value. Thus, $H_x(\eta,\xi)$ is almost independent of ξ, or correspondingly, $H_x(y)$ is independent of z in rectangular slots (Eq. (10)). The expression for the electric field components E_ξ and E_η follow from Maxwell equation curl $H = +i\omega\varepsilon_o E$

$$E_\xi(\xi,\eta) = -\frac{iZ_o}{kg}\frac{\partial H_x}{\partial \eta} = -i\frac{Z_o}{kg}C\,ce_1'(\eta,q)\left[Ce_1(\xi,q) + \frac{C_2}{C_1}Fey_1(\xi,q)\right] \tag{15}$$

$$E_\eta(\xi,\eta) = \frac{iZ_o}{kg}\frac{\partial H_x}{\partial \xi} = i\frac{Z_o}{kg}C\,ce_1(\eta,q)\left[\frac{\partial Ce_1(\xi,q)}{\partial \xi} + \frac{C_2}{C_1}\frac{Fey_1(\xi,q)}{\partial \xi}\right] \tag{16}$$

with $g = \left(c_o/\sqrt{2}\right)\sqrt{\cosh 2\xi - \cos 2\eta}$, the elliptical metric factor. The arc lengths ds_1 and ds_2, the hyperbolic and elliptic arc lengths, respectively are

$$ds_1 = g\,d\xi \quad \text{and} \quad ds_2 = g\,d\eta \tag{17}$$

Note that ds_1 being perpendicular to the elliptic contour ξ = const corresponds to changes across the gap (dz in [2]) and ds_2 is perpendicular to hyperbolic lines η = const (dy in [2]). Differentiating $Ce_1(\xi,q)$ with respect to ξ yields from Eqs. (14a) and (b):

$$\frac{\partial Ce_1(\xi,q)}{\partial \xi} = -\frac{ce_1'\left(\frac{\pi}{2},q\right)}{\sqrt{q}} \cdot 2\sqrt{q}\sinh\xi\left[\frac{\partial J_1(\rho)}{\partial \rho} - \frac{A_3^1}{A_1^1}\frac{\partial J_3(\rho)}{\partial \rho} + \cdots\right] \tag{18a}$$

$$\frac{\partial Fey_1(\xi,q)}{\partial\xi} = -\frac{ce_1'\left(\frac{\pi}{2},q\right)}{\sqrt{q}}\cdot 2\sqrt{q}\sinh\xi\left[\frac{\partial N_1(\rho)}{\partial\rho} - \frac{A_3^1}{A_1^1}\frac{\partial N_3(\rho)}{\partial\rho} + \cdots\right] \tag{18b}$$

with

$$\rho = 2\sqrt{q}\cosh\xi,\ \frac{\partial J_1(\rho)}{\partial\rho} = J_o(\rho) - \frac{J_1(\rho)}{\rho};\ \frac{\partial J_3}{\partial\rho} = J_2(\rho) - \frac{3}{\rho}J_3(\rho)$$

etc. Because, in the 30 GHz case, $\sinh\xi \approx 0.03345$, $\left|E_\eta\right| << \left|E_\xi\right|$. However, the tangential component of E is E_η on the elliptical surface ξ_0. Eq. (18) shows that $E_\eta = 0$ only for $\xi = 0$, that is on the confocal line. Because $\xi << 0$, $\sinh\xi \approx \xi$ is very small but not zero. To force E_η to be rigorously zero on ξ_0 we have to force the brackett of Eq. (16) to become zero on the surface $\xi = \xi_0$. Thus:

$$\left.\frac{\partial Ce_1(\xi,q)}{\partial\xi}\right|_{\xi_o} + \frac{C_2}{C_1}\left.\frac{\partial Fey_1(\xi,q)}{\partial\xi}\right|_{\xi_o} = 0 \tag{19}$$

Note that when $\xi = 0$, the argument of N becomes simply $2\sqrt{q} = kc_o/2$, regular and finite.

The constant $C_{(2)}$ is determined from the requirement (Eq. (19))

Observe that the Bessel expansion in Eq. (18b) is the same as that for Ce_1 given in Eq. (14a) since both, the J_n and N_n functions have the same recurrance relations. It then follows from Eq. (19)

$$-\frac{ce_1'\left(\frac{\pi}{2},q\right)}{\sqrt{q}}\frac{\partial}{\partial\xi}\left\{C_{(1)}\left[J_1\left(kc_o\cosh\xi\right) - \frac{A_3^1}{A_1^1}J_3\left(kc_o\cosh\xi\right) - +\cdots\right]\right.$$
$$\left. + C_{(2)}\left[N_1\left(kc_o\cosh\xi_o\right) - \frac{A_3^1}{A_1^1}N_3\left(kc_o\cosh\xi\right) + \frac{A_5^1}{A_1^1}N_5\left(kc_o\cosh\xi\right) - +\cdots\right]\right\}_{\xi=\xi_o} = 0 \tag{20}$$

or

$$kc_o\sinh\xi_o\left\{C_{(1)}\left[J_1'\left(kc_o\cosh\xi_o\right) - \frac{A_3^1}{A_1^1}J_3'\left(kc_o\cosh\xi_o\right) + \frac{A_5^1}{A_1^1}J_5'\left(kc_o\cosh\xi_o\right) - +\right]\right.$$
$$\left. + C_{(2)}\left[N_1'\left(kc_o\cos\xi_o\right) - \frac{A_3^1}{A_1^1}N_3'\left(kc_o\cosh\xi_o\right) + \frac{A_5^1}{A_1^1}N_5'\left(kc_o\cosh\xi\right) - +\right]\right\} = 0 \tag{21}$$

In Eq. (21) the prime over the Bessel functions designates the "ξ" derivative. Equation (21) is not an eigenvalue problem and it must be satisfied for all frequencies, that is regardless of the value of $kc_o = (\omega/c)c_o$. Since, as discussed earlier, $\sin h\xi_o \neq 0$, the expression in the wave brackets must vanish.

We have then, using $\rho_o = kc_o \cosh\xi_o \cong kc_o$

$$C_2(q) = -C_1(q)\frac{J_1'(\rho_o) - \frac{A_3'}{A_1'}J_3'(\rho_o) + \frac{A_5'}{A_1'}J_5'(\rho_o) - +....}{N_1'(\rho_o) - \frac{A_3'}{A_1'}N_3'(\rho_o) + \frac{A_5'}{A_1'}N_5'(\rho_o) - +....} \tag{22}$$

The coefficients A_1', A_3', $A_5', \cdots, A_{2r+1}'$ may be obtained from recurrence relations as given in [1] and [3]: The relation for the desired function $ce_1(\eta, q)$ and $r \geq 1$ is

$$(a_1 - 1 - q)A_1^1 - qA_3^1 = 0 \tag{23a}$$

$$\left[a_1 - (2r+1)^2\right]A_{2r+1}^1 - q\left(A_{2r+3}^1 + A_{2r-1}^1\right) = 0 \tag{23b}$$

For $q < 1$, the series converges rapidly and the required ratios A_{2r+1}^1/A_1^1 are easily obtained for a given value a_1—the characteristic number (separation constant) which are listed in [1] and [3]. The required expression for a_1 is

$$a_1 = 1 + q - \frac{q^2}{8} - \frac{q^3}{64} - \frac{1}{1536}q^4 \cdots \tag{24}$$

Then

$$\frac{A_3^1}{A_1^1} = -\left(\frac{q}{8} + \frac{q^2}{64} + \frac{q^3}{1536} + \cdots\right) \tag{25}$$

Table I lists the values of a_1, A_3^1, A_5^1 for a range of kc_o values as parameters. As q changes with frequency, the ratios are best computed as functions of q. Nevertheless, for $q_{max} \leq \pi^2/16$, $A_3^1/A_1^1 \approx q/8$; $A_5^1/A_1^1 \approx q^2/192$ to demonstrate the rapid decay of coefficients A_{2r+1} with increasing r. The derivatives of the $J(\rho)$ and $N(\rho)$ functions with regard to the argument are $\left(\left[Z(\rho)\right.\right.$ either $J(\rho)$ or $\left.\left.N(\rho)\right]\right)$:

$$\frac{dZ_n(\rho)}{d\rho} = -\frac{n}{\rho}Z_n(\rho) + Z_{n-1}(\rho) \tag{26}$$

Equation (22) may then be evaluated. As an example for $kc_o \approx kh = 1.4$ and $\xi_o = 0.03345$, $\rho \cong 1.4$, one gets $C_{(2)} \cong -0.1851\ C_{(1)}$. One should keep in mind, however, that $C_{(2)} = C_{(2)}(q)$, that is $C_{(2)}$ depends on frequency. This is also true of the coefficients $A_r(q) = A_r\left(k^2 c_o^2/4\right)$. Thus, the $C_{(1)}$, $C_{(2)}$, and the A_r's have to be computed as function of q. Table II shows the dependence on q of some important parameters and Bessel and Neumann functions to demonstrate their behavior. Note that for $q < 1$, that is of interest in this study, $\left|A_5^1\right| << \left|A_3^1\right| << \left|A_1^1\right|$ and the Bessel-Neumann series in the Eqs. (20), (21), (23), and others converge rapidly. Nevertheless, the expressions are cumbersome and for practical evaluation programming becomes indispensable.

We are turning now to the important expression for $E_\xi(\xi,\eta)$ that has to be matched at the gap $y = 0^-$ or $\eta = kh$ to the E_z component of $y = 0+$. From Eqs. (12) and (15)

$$E_\xi(\xi,\eta) = -i\frac{Z_o}{kg}\frac{\partial H_x}{\partial \eta} = -i\frac{Z_o}{kg}ce_1'(\eta,q)C_{(1)}\left[Ce_1(\xi,q) + \frac{C_{(2)}}{C_{(1)}}Fey_1(\xi,q)\right] \tag{27}$$

and $ce_1'(\eta,q) = \partial ce_1(\eta,q)/\partial\eta$. We have to normalize the parameter $C_{(1)} = C_{(1)}(q)$ such that for $\eta = kh$:

$$-i\frac{Z_o}{kg}ce_1'(kh,q)C_{(1)}[\ ] = E_o \tag{28}$$

The [ ] bracket designates the Bessel functions summations in Eq. (27)

$$C_{(1)} = i\frac{E_o}{Z_o}\frac{kc_o}{ce_1'(kh,q)\cdot[\ ]} \tag{28a}$$

At the center of the gap $\xi = 0$. The value of $\eta = kh$ at $y = 0^-$ is close to $kh = \pi/2$. Let us put $\eta = kh = \frac{\pi}{2} - \theta$, with $\theta << 1$. Then:

$$g = \frac{c_o}{\sqrt{2}}\sqrt{\cosh 2\xi - \cos 2\eta} \approx c_o\sqrt{1 - \frac{\theta^2}{2}} \approx c_o\left(1 - \theta^2/2\right) \approx c_o$$

and kg in Eq. (28) becomes $kg \approx kc_o$. As discussed in the introduction the assumption $E = E_o$ in the gap is better than 98 percent accurate for narrow gaps and $h >> \delta$. Using $C_{(1)}$ from Eqs. (28) and (12) one gets

$$H_x(\xi,\eta) = -i\left(\frac{E_o}{Z_o}\right)(kc_o)\frac{ce_1(\eta,q)}{ce_1'(\eta,q)} \tag{12a}$$

$$-ce_1'(\eta,q)_{\eta=kh} = \sin kh\left[1-\frac{3}{8}q\left(1+\frac{q}{8}+\frac{q^2}{192}+\cdots\right)\frac{\sin 3kh}{\sin kh}+\frac{5}{192}q^2\left(1+\frac{q}{6}\cdots\right)\frac{\sin 5kh}{\sin kh}\ \cdots\right]$$

$$= \sin kh\left[1-3\alpha_3\frac{\sin 3kh}{\sin kh}+5\alpha_5\frac{\sin 5kh}{\sin kh}-+\cdots\right] \tag{29}$$

The dispersion relation (Eq. (1.67) or (1.79) in [2]) is obtained in our case by matching H_x^+ to H_x^- as given by Eq. (12a) at the boundary of the gap, given by $\eta = kh$. Using Eq. (1.65) [2]

$$H_x^+ = i\frac{k}{Z_o}E_o\sum_{n=-\infty}^{+\infty}\frac{M_n}{\gamma_n}e^{-i\beta_n z}e^{i\beta_n\frac{\delta}{2}} \tag{30}$$

and taking, as discussed earlier $z = \delta/2$, the center of the gap $(\xi = 0)$ and H_x^- from Eq. (12), one gets:

$$kc_o\cdot\frac{ce_1(kh,q)}{-ce_1'(kh,q)} = k\sum_{n=-\infty}^{+\infty}\frac{M_n}{\gamma_n}\cdot\frac{\delta}{L} \tag{31}$$

$$(\cot kh)f(kh,q) = \left(\frac{\cos kh}{\sin kh}\right)\frac{\left[1-\alpha_3(q)\frac{\cos 3kh}{\cos kh}+\alpha_5(q)\frac{\cos 5kh}{\cos kh}-+\right]}{1-3\alpha_3\frac{\sin 3kh}{\sin kh}+5\alpha_5\frac{\sin 5kh}{\sin kh}-+} = \frac{\delta}{L}\sum_{n=-\infty}^{+\infty}\frac{M_n}{\gamma_n c_o} \tag{32}$$

where $\alpha_3(q), \alpha_5(q)\cdots$ are the coefficients of the cosine expansions given in Eq. (13). We now rewrite Eq. (32)

$$c_o\cot kh\cdot f(q,kh) = \frac{\delta}{L}\frac{M_o}{\gamma_{oe}}\left[1+\sum_{n\neq 0}\frac{M_n/M_o}{\gamma_{ne}/\gamma_{oe}}\right] = \frac{\delta}{L}\frac{M_o}{\gamma_{oe}}\left[1+\frac{M_{-1}/M_o}{\gamma_{-1}/\gamma_o}+\frac{M_1/M_o}{\gamma_{-1}/\gamma_o}+\frac{M_{-2}/M_o}{\gamma_{-2}/\gamma_o}+\frac{M_2/M_o}{\gamma_2/\gamma_o}+\cdots\right]$$

(33)

For large n, $M_n \approx (\sin n\pi\cdot\delta/L)/(n\pi\cdot\delta/L) \to 0$ and $\gamma_n \approx \beta_n \to 2\pi n\delta/L \to \infty$

Further rearranging of Eq. (33) gives

$$\gamma_{oe}c_o \approx \gamma_{oe}h = \frac{\delta}{L}M_{oe}\left[1+\sum_{n\neq 0}\frac{M_{ne}/M_{oe}}{\gamma_{ne}/\gamma_{oe}}\right]\frac{\tan kh}{f(kh,q)}. \tag{34}$$

The subscript "e" denotes quantities belonging to "elliptic" solutions. The function $f(kh,q)$ is equal to 1 as $k = \omega/c \to 0$ because $q = k^2c_o^2/4$ goes to zero as ω^2 and $\alpha_3, \alpha_5, \cdots$ also become zero. It also equals 1 as $kh \to \pi/2$ and has as shallow maximum around 1.08 at $kh \approx \pi/4$. Around the selected design point $kh \approx 1.45$, $f = 1.01 \approx 1$. Comparing Eq. (34) with Eq. (1.67) [2]

$$\frac{1}{\tan kh} = k \cdot \frac{\delta}{L}\sum \frac{M_n}{\gamma_n} = \frac{\delta}{L} kh \frac{M_o}{\gamma_o h} h\left[1 + \sum_{n\neq 0} \frac{M_n/M_o}{\gamma_n/\gamma_o}\right] \tag{1.67}$$

or

$$\gamma_o h = \frac{\delta}{L} kh \tan kh\, M_o\left[1 + \sum_{n\neq 0} \frac{M_n/M_o}{\gamma_n/\gamma_o}\right] \tag{1.67}$$

and assuming that the sums in the square bracket are not much different from each other in both cases one obtains an approximate expression $\left(c_o = \sqrt{h^2 - \frac{\delta^2}{4}}\right)$

$$\gamma_{oe} \approx \gamma_o \frac{h}{\sqrt{h^2 - \frac{\delta^2}{4}}} \frac{1}{f(kh,q)\cdot kh} \tag{35}$$

From Eq. (35) it follows

$$\beta_{oe} \approx \sqrt{k^2 + \frac{h^2}{c_o^2}\frac{\gamma_o^2}{f^2 \cdot (kh)^2}} \tag{36}$$

The plots $\beta_o L/\pi$ and $\beta_{oe} \cdot L/\pi$ versus kh as ordinate are shown in Fig. 3. Expression (36) is a good approximation when $\eta = kh \approx \pi/2$, then $\cos 2\eta = \cos \pi = -1$ and $g = c_o/\sqrt{2}\ \sqrt{\cosh 2\varsigma + 1} = c_o \cosh \varsigma \equiv c_o$. The case $kh \approx \pi/2$ is of interest for low voltage designs because then $h \approx \lambda_o/4$. When η is much less than $\pi/2$, then

$$g = \frac{c_o}{\sqrt{2}}\sqrt{\cosh 2\xi - \cos 2kh} \approx \frac{c_o}{\sqrt{2}}\sqrt{1 - \cos 2kh} = \frac{c_o}{\sqrt{2}}\sqrt{2\sin^2 kh} \approx c_o \sin kh$$

because $0 < \xi < \xi_o << 1$ and $\cosh 2\xi_o \approx 1 + 2\,\xi_o^2 \approx 1$. In the general case, the matching of H_x^- to H_x^+ at $\xi = 0$ is accomplished by the expression

$$i\frac{E_o}{Z_o}(\cot kh)kg\frac{1 - \alpha_3\frac{\cos 3kh}{\cos kh} + \alpha_5\frac{\cos 5kh}{\cos kh} - +\cdots}{1 - 3\alpha_3\frac{\sin 3kh}{\sin kh} + 5\alpha_5\frac{\sin 5kh}{\sin kh}} = i\frac{E_o}{Z}k\frac{\delta}{L}\sum_{n=-\infty}^{+06}\frac{M_n}{\gamma_n} \tag{37}$$

or

$$\frac{g}{tan\, kh}\cdot f(kh,q) = \frac{\delta}{L}\sum_{\text{all } n}\frac{M_n}{\gamma_n} = \frac{\delta}{L}\frac{M_o}{\gamma_o}\sum_{n\neq 0}\left(1 + \frac{M_n/M_o}{\gamma_n/\gamma_o}\right) \tag{37a}$$

At $\xi = 0$, $g = \frac{c_o}{\sqrt{2}}\sqrt{2\sin^2 kh} = c_o \sin kh$, Eq. (37a) becomes

$$\frac{c_o \sin kh \cdot \cos kh}{\sin kh} f(kh,q) = \frac{\delta}{L}\frac{M_o}{\gamma_o}\sum_{n\neq 0}\left(1+\frac{M_n/M_o}{\gamma_n/\gamma_o}\right) \tag{38}$$

Equation (38) is always accurate when $\xi = 0$ at the center of gap. As mentioned earlier, a rigorous evaluation of Eq. (1.67) as described by Collins [4] indicates that the $M_o = \left[\sin\beta_o(\delta/2)\right]/\left[\beta_o(\delta/2)\right]$ should be replaced by M_o^2 which, for small gaps, amounts to 2 percent correction. Thus, the corrected formulae should be rewritten as

$$\frac{1}{kh\,\tan\,kh} = \frac{\delta}{L}\sum_n \frac{M_n^2}{\gamma_n} = \frac{\delta}{L}\frac{M_o^2}{\gamma_n}\sum_{n\neq 0}\left(1+\frac{M_n^2/M_o^2}{\gamma_n/\gamma_o}\right) \tag{1.67a}$$

for rectangular slots [2] and

$$c_o \cos kh = \frac{1}{f(kh,q)}\frac{M_{oe}^2}{\gamma_{oe}}\frac{\delta}{L}\sum_{n\neq 0}\left(1+\frac{M_{ne}^2/M_{oe}^2}{\gamma_{ne}/\gamma_{oe}}\right) \tag{38a}$$

as more correct expressions for the dispersion relation.

Power Dissipation in the Elliptical Slot

The expression for the power dissipated on the walls of the elliptical cylinder is given by

$$P_D = \frac{R'_{\square}}{2}\iint \left|H_{\tan}(\eta,q)\right|^2_{\xi=\xi_o} g\,d\eta\,dx = R'_{\square}\,\frac{w}{2}\int \left|H_\eta(\eta,q)\right|^2_{\xi=\xi_o} g\,d\eta \tag{39}$$

$$\left(R'_{\square}[\Omega] = 34\sqrt{\rho/\lambda};\ \rho[\Omega cm],\ \lambda[cm]\right):$$

For small values $\xi_o << 1$, the ratio $Ce_1(\xi_o,q)/Ce_1(0,q)$ in Eq. (12a) may be taken as 1 with an error of 0.2 percent in the worst case and

$$\left|H_x(\eta,q)\right|^2 = \left(\frac{E_o}{Z_o}\right)^2 (kc_o)^2\,\frac{ce_1^2(\eta,q)}{\left[ce_1'(kh,q)\right]^2} \tag{40}$$

With $g = c_o/\sqrt{2}\,\sqrt{\cos h\,2\xi - \cos 2\eta}$ Eq. (39) becomes at $\xi = \xi_o$

$$P_D = \frac{R'_{\square}}{2}\left(\frac{E_o}{Z_o}\right)^2 (kc_o)^2 \Big/ \left[ce_1'(kh,q)\right]^2 \cdot \frac{wc_o}{\sqrt{2}}\int_0^{\pi h} ce_1^2(\eta,q)\sqrt{\cos h\,2\xi_o - \cos 2\eta}\,d\eta \tag{41}$$

$$= \frac{R'_{\square}}{2}\left(\frac{E_o}{Z_o}\right)^2\left(\frac{kc_o}{ce_1'(kh,q)}\right)^2 \frac{wc_o}{\sqrt{2}}\int_0^{kh} ce_1^2(\eta,q)\sqrt{\cos h\,2\xi_o}\sqrt{1-\frac{\cos 2\eta}{\cos h\,2\xi_o}}\,d\eta \qquad (41a)$$

The expression $\sqrt{1-\cos 2\eta/\cos h\,2\xi_o}$ leads to elliptic integrals which are well tabulated or easily computed, but do not yield a useful closed form formula. To examine the behavior of the integral in Eq. (41) let us rewrite

$$\sqrt{\cos h\,2\xi_o - \cos 2\eta} = \sqrt{1 + 2\xi_0^2 + \frac{2}{3}\xi_0^4 - 1 + 2\sin^2\eta + \ldots} \qquad (42)$$

Now the ratio $\frac{b}{a}$, the minor to major half axes, equals to

$$\frac{b}{a} = \frac{\delta/2}{h} = \frac{\sin h\xi_o}{\cos h\xi_o} = \tan h\xi_o.$$

For the 30 GHz Forward Wave TWT at 6kV: $\delta/2h = 1/30$, and $\xi_o = 0.0333$. For a high power Forward TWT magnetron amplifier $\xi_o \lessapprox 0.06$. The highest ratio $\delta/2h \approx 0.25$ appears in the designs for 1THZ BWO, with the resulting value $\xi_o \approx 0.25$. The value of the intergral in Eq. (41) is then approximately 10% larger than that obtained with negligible ξ_o. Due to the smallness of ξ_0^2 the integral and the integrand in Eq. (41) will be different only when $\sin\eta \lesssim \xi_0$. Figures 4(a) and (b) show computed values of $F(x,\xi) = \int_0^x \sqrt{\xi_0^2 + \sin^2\eta}\;d\eta$ with $\xi_0 = 0.25$ and 0.0666 and $I(x) = \int_0^x \sin\eta\,d\eta = -\cos\eta\Big|_0^x$.

For $\xi_0 = 0.06$, at $x = 0.2$; $F(x,\xi) = 0.025062$ and $I(x) = 0.01993342$ or an error of 20 percent. But at $kh \cong 1.5$, the actual upper integration limit, $F(x,\xi) \approx 0.94$ an error of only 1 percent. Thus, in computing the total loss we are justified to neglect ξ_0^2 in Eq. (33). Then:

$$P_D = R'_{\square}\frac{1}{2}\left(\frac{E_o}{Z_o}\right)^2 wc_o\int_0^{\kappa h} ce_1^2(\eta,q)\sin\eta\,d\eta \qquad (43a)$$

Using Eq. (13) for $q_{max} \le 0.5625$; $q^2 < 0.316$; etc. we may neglect higher powers in q and α. $ce_1^2(\eta,q)$ then becomes

$$ce_1^2(\eta,q) = \cos^2\eta\left[1 - \alpha_3\frac{\cos 3\eta}{\cos\eta} + \alpha_5\frac{\cos 5\eta}{\cos\eta} - +\cdots\right]^2$$

$$= \cos^2\eta\left[1 - 2\alpha_3\left(4\cos^2\eta - 3\right) + 2\alpha_5\left(\cos^4\eta - 10\sin^2\eta\cos^2\eta + 5\sin^{-2}\eta\right) + -\cdots\right]$$

$$\approx \cos^2\eta\left(1 - 8\alpha_3\cos^2\eta + 6\alpha_3\right) \qquad (44)$$

inserting Eq. (44) into the integral in Eq. (43a):

$$\int_0^{\kappa h} ce_1^2(\eta,q)\sin\eta\,d\eta \approx \int_0^{\kappa h}\cos^2\eta\sin\eta\left(1-8\alpha_3\cos^2\eta+6\alpha_3\right)d\eta$$

$$\equiv -\frac{\cos^3\eta}{3}\left(1+6\alpha_3\right)\Big|_0^{kh}+\frac{8}{5}\alpha_3\cos^5\eta\Big|_0^{kh}=\frac{1+6\alpha_3}{3}\left(1-\cos^3 kh\right)+\frac{8}{5}\alpha_3\left(\cos^5 kh-1\right) \tag{45}$$

Integration from 0 to kh gives the approximate power loss on one side. Using Eq. (43a) for two sides one gets:

$$P_{De}=\frac{1}{2}\cdot 2\cdot R_{\square}'\left(\frac{E_o}{Z_o}\right)^2\left(\frac{kc_o}{ce_1'(kh,q)}\right)^2 wc_o\left[\frac{1+6\alpha_3}{3}\left(1-\cos^3 kh\right)+\frac{8}{5}\alpha_3\left(\cos^5 kh-1\right)\right]$$

$$=\frac{R_{\square}'}{3}\left(\frac{E_o}{Z_o}\right)^2\left[\frac{kc_o}{ce_1'(kh,q)}\right]^2 wc_o\left[\left(1+6\alpha_3\right)\left(1-\cos^3 kh\right)+\frac{24}{5}\alpha_3\left(\cos^5 kh-1\right)\right] \tag{46}$$

From Eq. (29)

$$\left[ce_1'(kh,q)\right]^2 \approx \sin^2 kh\left[1-3\alpha_3\frac{\sin 3kh}{\sin kh}+5\alpha_5\frac{\sin 5kh}{\sin kh}-+\cdots\right]^2$$

$$\approx \sin^2 kh\left(1-6\alpha_3\frac{\sin 3kh}{\sin kh}+9\alpha_3^2\frac{\sin^2 3kh}{\sin^2 kh}\right) \tag{47}$$

if $a_5 << \alpha_3$ as well as products $\alpha_3\cdot\alpha_5$ are neglected. Now, at the operational point of interest $kh = 1.4$ to 1.5 and $\sin kh \approx 1$; $\sin 2kh \approx 0.1$ and $\sin 3kh \approx -1$; thus, for $kh \approx 1.5$, Eq. (47) becomes

$$\left[ce_1'(1.5,q)\right]^2 \approx \left(1+6\alpha_3+9\alpha_3^2\right)\sin^2 kh$$

and Eq. (46) becomes approximately

$$P_{De}\Big| \approx \frac{R_{\square}'}{3}\left(\frac{E_o}{Z_o}\right)^2\frac{\left(kc_o\right)^2 wc_o}{\sin^2 kh}\left(1-4.8\alpha_3\right) \tag{48}$$

The corresponding result for rectangular slots of equal width w and height h and gap δ is

$$P_{DR} = 2\frac{R_{\square}'}{\sin^2 kh}\left(\frac{E_o}{Z_o}\right)^2 wh\left[1+\frac{\sin 2kh}{2kh}+\frac{\delta}{h}\right] \tag{49}$$

Equating Eqs. (48) and (49):

$$\frac{1}{3}\left(kc_o\right)^2 wh\sqrt{1-\frac{\delta^2}{4h^2}}=\frac{1}{2}\frac{wh\left[1+\frac{\sin 2kh}{2kh}+\frac{\delta}{h}\right]}{\sin^2 kh\left(1-4.8\alpha_3\right)} \tag{50}$$

or

$$kc_o \approx \frac{\sqrt{\frac{3}{2}}\sqrt{1+\frac{\sin 2kh}{2kh}+\frac{\delta}{h}}}{\sqrt{\left(1-4.8\alpha_3\right)}} \approx 1.53 \tag{50a}$$

For the ratio P_{DR}/P_{De} it then follows from Eqs. (46) and (49)

$$\frac{P_{DR}}{P_{De}} \approx \frac{3}{2}\cdot\frac{h}{c_o}\frac{1+\frac{\delta}{h}+\frac{\sin 2kh}{2kh}}{\left(kc_o\right)^2}\frac{1-6\alpha_3\frac{\sin 3kh}{\sin kh}+9\alpha_3^2\frac{\sin 3kh}{\sin^2 kh}}{\left(1+6\alpha_3\right)\left(1-\cos^3 kh\right)+\frac{24}{5}\alpha_3\left(\cos^2 kh-1\right)} \tag{51}$$

Thus, below approximately $kc_O \approx 1.53$ the losses of an elliptical cylinder are smaller than those of an equivalent rectangular counterpart. Moreover, they decrease roughly as $\left(kc_o\right)^2 = k^2h^2\left[1-\left(\delta^2/4h^2\right)\right]$ decreases. For a given frequency k it means either a decrease in h (higher voltage) or increase in δ (gap width). The former is of interest to traveling wave magnetrons, since reduced losses result in lower noise output and for BWO's at harmonic frequencies, where increasing δ/h is a necessity.

Since the α coefficients are functions of frequency, accurate evaluation of Eq. (46) and others requires extensive programming and computation work. The power losses in the space above $y = 0$ are identical to those obtained in rectangular coordinates.

Stored Energy in the Elliptical Slot

Since $H_x(\xi,\eta)$ is the only magnetic field component, the stored energy is given by

$$W_e = 2\frac{\mu_o}{2}\int_0^w\int_0^{\xi_o}\int_0^{\kappa h}\left|H(\xi,\eta)\right|^2 g^2 d\xi\, d\eta\, dx \tag{52}$$

because integration from 0–ξ_0 covers only one half of the elliptical slot.

For small $\xi << 1$, we neglect the dependence of H on ξ as discussed earlier (see Eq. (14)) and obtain

$$W_e = \mu_o\frac{wc_0^2}{2}\int_{\xi=0}^{\xi_0}\int_{\eta=0}^{kh}\left(\frac{E_o}{Z_o}\right)^2\left(kc_o\right)^2\frac{ce_1^2(\eta,q)}{\left|ce_1'(kh,q)\right|^2}(\cosh 2\xi-\cos 2\eta)d\xi\, d\eta \tag{53}$$

$$= \mu_o w \frac{(kc_o)^2 \cdot \frac{c_0^2}{2}}{\left|ce_1'(kh,q)\right|^2}\left(\frac{E_o}{Z_o}\right)^2$$

$$\times\left[\int_{\xi=0}^{\xi_o}\cosh 2\xi\, d\xi \int_{\eta=0}^{\kappa h} ce_1^2(\eta,q)d\eta - \int_0^{\xi_o} d\xi \int_0^{\kappa h} ce_1^2(\eta,q)\cos 2\eta\, d\eta\right] \tag{54}$$

$$= \mu_o\left(\frac{E_o}{Z_o}\right)^2 \frac{c_0^2}{2} w \frac{(kc_o)^2}{\left|ce_1'\right|^2}\left[\frac{\sinh 2\xi_o}{2}\int_0^{\kappa h} ce_1^2(\eta,q)d\eta - \xi_o\int_0^{\kappa h} ce_1^2(\eta,q)\cos 2\eta\, d\eta\right] \tag{55}$$

$$= \frac{\mu_o}{2}\left(\frac{E_o}{Z_o}\right)^2\left(\frac{kc_o}{ce_1'}\right)^2 \frac{c_0^2}{2} w\left[\sinh\xi_o\cosh\xi_o\int_0^{\kappa h}\left\{\cos^2\eta\left(1+6\alpha_3\right) - 8\alpha_3\cos^4\eta + \right.\right.$$

$$\left.\left. 2\alpha_3\ \left(\cos^4\eta - 10\sin^2\eta\cos^2\eta + 5\sin^2\eta\right)\right\}d\eta - \xi_o\int_0^{\kappa h} ce_1^2(\eta,q)\cos 2\eta\, d\eta\right] \tag{55a}$$

In developing Eq. (55a) higher powers of α_3 and α_5 were neglected for simplicity, α_3 being < 1/16, $\alpha_3^2 \le 1/256$ and $\alpha_5 \le 1/192$ in the worst case. When integration of the terms in Eq. (55a) is performed, the following results:

$$W_e = \frac{\mu_o}{4}\left(\frac{E_o}{Z_o}\right)^2 \frac{(kc_o)^2}{\left(ce_1'\right)^2} w\left\{c_o\sinh\xi_o c_o\cosh\xi_o\,\frac{kh}{2}\left(1+\frac{\sin 2kh}{2kh} - 4\alpha_3\frac{\sin 2kh}{2kh}\cos^2 kh\right)\right.$$

$$\left. -c_0^2\xi_o\frac{kh}{4}\left(1+\frac{\sin 2kh}{2kh}+\frac{\sin 4kh}{4kh}\right) + \alpha_3 c_0^2\xi_o\frac{kh}{2}\left(1-3\frac{\sin 4kh}{4kh} - \frac{1}{3}\frac{\sin^3 kh}{kh}\right)\right\} \tag{56}$$

Except for having neglected higher order terms of α, Eq. (56) is an accurate expression for W_e.

Recall that $c_o\sinh\xi_o = \delta/2 =$ half of the minor axis and $c_o\cosh\xi_o = h =$ half of the major axis and that

$$\int_0^{\xi_o}\int_0^{2\pi} g^2 d\xi\, d\eta = \int_0^{\xi_o}\int_0^{2\pi}\frac{c_0^2}{2}(\cosh 2\xi - \cos 2\eta)d\xi\, d\eta$$

$$= \frac{c_0^2}{2}\int_0^{\xi_0}\cosh 2\xi\, d\xi\cdot 2\pi - \frac{c_0^2}{2}\xi_0\int_0^{2\pi}\cos 2\eta\, d\eta \tag{57}$$

$= \frac{c_0^2}{2}\cdot\sinh\xi_o\cosh\xi_o\cdot 2\pi = \pi\cdot h\cdot\delta/2 =$ area of an ellipse, because the second integral in Eq. (57) is zero. Let us examine the result in Eq. (56). Since $\sinh\xi_0$ and $\cosh\xi_0$ may be expanded in a series and for $\xi << 1$ the series converges rapidly, Eq. (56) may be presented in the form:

$$W_e = \frac{\mu_o}{2}\left(\frac{E_o}{Z_o}\right)^2 \frac{(kc_o)^2}{(ce_1')^2} w c_0^2 \xi_o \frac{kh}{4}\left[1 + 2\alpha_3 \frac{\sin 2kh}{kh} + \frac{\sin 4kh}{4kh}\right] \tag{58}$$

Let us compare Eq. (58) with the simplest form of stored energy in rectangular slot of height h and width δ

$$W_R = \frac{\mu_o}{4}\left(\frac{E_o}{Z_o}\right)^2 \cdot \frac{\delta h \cdot w}{\sin^2 kh}\left(1 + \frac{\sin 2kh}{2kh}\right) \tag{59}$$

Taking the ratio of Eqs. (49) and (48) one gets approximately

$$\frac{W_R}{W_e} \approx 2\frac{[ce_1'(kh,q)]^2}{(kc_o)^2(kh)} \frac{\delta h}{c_0^2 \xi_o} \frac{\left(1 + \frac{\sin 2kh}{2kh}\right)}{\sin^2 kh} \tag{60}$$

$$\approx 2\frac{\delta}{(kc_o)^3 \cdot c_o \xi_o} \frac{1 + 6\alpha_3 + \frac{\sin 2kh}{2kh}}{1 + 2\alpha_3 + \frac{\sin 4kh}{4kh}} \tag{60a}$$

But $\delta/2 = c_o \sinh \xi_o \approx c_o \xi_o$ for $\xi_o << 1$, and then

$$\frac{W_R}{W_e} \approx \frac{4}{(kc_o)^3} \frac{1 + \frac{\sin 2kh}{2kh} + 6\alpha_3}{1 + 2\alpha_3 + \frac{\sin 4kh}{4kh}} \tag{60b}$$

For $kc_o \lesssim 2$, the numerical value of Eq. (60b) is larger than 1, a significant fact, that impacts the interaction impedance toward higher values in elliptical slots. When the slots become less deep, $kc_o = 1$, $W_R/W_e \gtrsim 4$ indicating large improvements in impedance. The stored energy above the slots $0 \le y \le d$ is identical to that obtained in rectangular coordinates, designated W_u

$$W_u = \frac{\varepsilon_o}{4} Ldw E_0^2 \sum_{n=-\infty}^{+\infty} \frac{k^2}{\gamma_n^2} M_n^2 \frac{1 + \frac{\sinh 2\gamma_n d}{2\gamma_n d}}{\sinh^2 \gamma_n d} \tag{61}$$

The total stored energy required for computing of the interaction impedance is the sum of Eqs. (56) and (61). Note that

$$\mu_o \cdot \frac{E_0^2}{Z_0^2} = \mu_o \cdot \frac{\varepsilon_o}{\mu_o} E_0^2 = \varepsilon_o E_0^2.$$

DISCUSSION OF RESULTS

The analysis developed in this study took as an approximation only one wave downwards into the half elliptical slot represented by the $ce_1(\eta,q)$ function and its derivative $ce_1'(\eta,q)$. They correspond one by one to the simple TEM wave representation ($H \sim \cos ky$, $E \sim \sin ky$) in the rectangular slot which leads to $E_z \equiv E_0$ = constant across the gap and to an error of less than 2 percent, as discussed in the introduction. To include higher TM waves in elliptical coordinates would require taking all $ce_m(\eta,q)$ with corresponding $Ce_m(\xi,q)$ and $Fey_m(\xi,q)$ functions and obtain then an infinite by infinite secular determinant equal to zero. The resulting improvement in accuracy is probably in the same range of 1 to 2 percent. Most numerical results quoted in this study were obtained by neglecting α_5 and higher powers of $\alpha_3\left(\alpha_3^2,\ \alpha_3^3,\ \ldots\right)$. For $q \approx 0.5$ the errors are $q^2/64 \approx 1/256$ for each term. Altogether all the errors are likely to amount to 5 to 10 percent, an error still acceptable for comparative evaluations.

The virtual constancy of E_z across the gap δ is evident from

$$\nabla \cdot E = \frac{\partial E_y}{\partial y} + \frac{\partial E_z}{\partial z} = 0 .$$

When h >> δ and δ << λ_o, E_y being tangential to the slot wall is nearly zero inside. Then $\partial E_z / \partial z \equiv 0$ and $E_z \approx$ constant.

REFERENCES

[1] McLachlan, N.W.: Theory and Applications of Mathieu Functions. Oxford UK, at the Clarendon Press, 1947.

[2] Watkins, D.A.: Topics in Electromagnetic Theory. John Wiley & Sons, Inc., New York, 1958.

[3] Abramowitz, M.; and Stegun, I., eds.: Handbook of Mathematical Functions. N.B.S., Series 55, June 1964.

[4] Collins, R.E.: Foundations for Microwave Engineering. McGraw-Hill, New York, 1966.

[5] Gewartowski, J.W.; and Watson, H.A.: Principles of Electron Tubes. D. Van Nostrand Co., Inc., Princeton, NJ, 1965.

APPENDIX I

TRANSVERSE BEAM-WAVE COUPLING COEFFICIENT OF THE SLOTTED SLOW WAVE VANE STRUCTURE

Figure 5 shows a cross-section of a vane with height h and width w and a beam hole of radius $b << w$. The center of the hole is located at O′ or a distance $-y_o$ below the top of vanes, $y = 0$. In the simple (but very accurate) single TEM wave theory the electric field in the slots behaves as equation (9)

$$E_z(y) = E_o \frac{\sin k(h + y)}{\sin kh} e^{-i\beta_o mL} \tag{9}$$

We introduce now circular coordinates inside the beam hole with radius b centered at $y = -y_o$. Consider a narrow strip of thickness dy located at $y = -y_o + b\cos\alpha$. The half width $BA = b\sin\alpha$. The area of the strip dA is

$$dA = 2b\sin\alpha\, dy = -2b^2\sin^2\alpha\, d\alpha \tag{A1}$$

$$\cos\alpha = \frac{y + y_o}{b};\ \sin\alpha = \sqrt{1 - \left(\frac{y + y_o}{b}\right)^2} \tag{A2}$$

The area of the hole is, of course

$$A = -2b^2\int_{\pi}^{0}\sin^2\alpha\, d\alpha = \pi b^2$$

The magnitude of E_z at $y = -y_o + b\cos\alpha$ is:

$$\left|E_Z(y)\right| = E_o \frac{\sin k\left(h - y_o + b\cos\alpha\right)}{\sin kh} \tag{A3}$$

The transverse beam coupling coefficient M_2 is defined:

$$M_2^2 = \frac{1}{\pi b^2 E_o^2}\int E_Z^2\, dA = \frac{-2b^2}{\pi b^2\sin^2 kh}\int_{-y_o-b}^{-y_o+b}\left[1 - \left(\frac{y + y_o}{b}\right)^2\right]\sin^2 k(h + y)\, dy$$

$$= -\frac{2}{\pi\sin^2 kh}\int_{\pi}^{0}\sin^2\alpha\sin^2 k\left(h - y_o + b\cos a\right)d\alpha \tag{A4}$$

with

$$\sin k\left[\left(h - y_o\right) + b\cos\alpha\right] = \sin k\left(h - y_o\right)\cos\left(kb\cos\alpha\right) + \cos\kappa\left(h - y_o\right)\sin k(b\cos\alpha)$$

and, because $kb = (kh)\frac{b}{h} \equiv 0.15 < 1$, we may expand

APPENDIX II

A BRIEF LOOK AT THE SUBMILLIMETER BACKWARD WAVE OSCILLATOR IN ELLIPTICAL CROSS-SECTION SLOTS

To date the only successful BWO in the frequency range 500 to 2000 GHz is the vane structure (analyzed in this paper) as used in the first space harmonic with opposite group and phase velocities (see Fig. 6).

Let us examine the design parameters of such a backward mode for the rectangular slots. The favorable range lies at a phase shift $\beta L \approx 2\pi - \pi/3$ because the group velocity becomes much smaller than c and with it the coupling impedance increases to required values to permit the start of oscillations.

The phase velocity $v_{-1} = \omega/\beta_{-1}$ is obtained from

$$\beta_{-1} \cdot L = 2\pi - \beta_0 L \tag{A7}$$

with $\beta_o L$ chosen to be $\frac{\pi}{3}$ it follows

$$\beta_{-1} \cdot L = \frac{5}{3}\pi \tag{A8}$$

$$v_{-1} = \frac{\omega}{\beta_{-1}} = \frac{\omega L}{\frac{5}{3}\pi} \tag{A9}$$

Assume the choice of the beam voltage $V_o = 5000$ V. Then the electron velocity $u_o = 4.166.10^9$ cm/sec. For a frequency of oscillations $f = 1000$ GHz $= 10^{12}$ Hz one gets

$$v_{-1} = u_o = \frac{\omega L}{\frac{5}{3}\pi} \tag{A10}$$

$$L = u_o \frac{\frac{5}{3}\pi}{2\pi f} = \frac{5}{6}\frac{u_o}{f} = \frac{5}{6}\frac{4{,}166\cdot 10^9}{1\cdot 10^{12}} = 3.47\cdot 10^{-3} \text{ cm}$$

The operational point on the $kh = F(\beta L)$ dispersion curve has a value $kh \approx 1.4 = (\omega/c)h$ and

$$h = 1.4\frac{c}{2\pi f} = 6.684\cdot 10^{-3} \text{ cm} \tag{A11}$$

Thus $h/L = 1.926$ and because $\delta \approx L/2$

$$\frac{h}{L} = \frac{h}{2\delta} \approx 2; \frac{h}{\delta} \approx 4 \tag{A12}$$

If the slots were designed to have an elliptical cross section with the depth h (half major axis) and $c_o \approx \sqrt{h^2 - \delta^2/4} \approx h$ we obtain for the important parameter $kc_o \approx kh = 1.4$ and from Eq. (60b)

$$\frac{W_R}{W_e} \approx 2 \tag{A13}$$

Thus the stored energy of elliptic slots is almost two times smaller, or the interaction impedance approximately two times higher. To examine the impact of this result on the performance of the BWO we refer to Figs. 11.1-3 and 11.1-4 in [5] reprinted as Fig. 7. In Fig. 7 the parameter Q/N, the quotient of the space charge parameter Q and the number N of electronic wavelength on the structure is shown. Note that in the linear theory Q is independent of I_o!

$$Q = \frac{1}{C^3}\left(\frac{\omega_q}{2\omega}\right)^2 = \frac{1}{4C^3} R^2 \frac{\omega_p^2}{\omega^2} = R^2 \frac{\sqrt{\frac{e}{m}V_0}}{4\sqrt{2}\pi^3 b^2 \varepsilon_0 K f^2} \tag{A14}$$

where C is Pierce's gain parameter, ω_p the unreduced plasma frequency, $\omega_q = R \cdot \omega_p$, R being the plasma frequency reduction parameter, b the beam radius, and K the effective interaction impedance. Knowing Q from Eq. (A14) and assuming a range of values of N the value of $CN = (I_o \cdot K_{-1}/4V_o)^{1/3} \cdot N$ necessary to start oscillations has been plotted in Fig. 11.1-3. Knowing C, the necessary current I_o may be calculated.

An examination of the curves in Fig. 11.1-3 indicates a double benefit for the starting current as result of increased interaction impedance K_{-1}: First, increased value for K_{-1} reduces the value of the passive mode parameter Q according to Eq. (A14). For a selected value N and an assumed or measured value of loss decreasing Q moves the corresponding CN ordinate to lower values. Then, secondly, because $\omega_q = R \cdot \omega_p$ increasing K_{-1} decreases I_o, the starting current, such that the product $I_o K_{-1}$ remains constant. It appears, therefore, that doubling the impedance would reduce the required $I_{o\text{-start}}$ by a factor higher than two, a very valuable advantage. As an example, the Thompson-CSF made 1THz BWO which utilizes the very same vane circuit with rectangular slots, has the following design parameters at f = 1THz = 1000 GHz:

L = 40 μm

δ = 20 μm

h = 75 μm

N = 30

w = 90 μm

b = 22 μm (beam opening radius)

V_o = 7 kV; I_o = 22 mA;

J_D =1750 A/cm^2 (current density in the beam)

This extremely high requirement for current density imposes great difficulties on the cathode life and gun construction. Any relief by factor 2 or more would be highly beneficial and necessary.

TABLE I.

kc	$q=\frac{k^2c_0^2}{4}$	a_1	A_3'/A_1'	A_1'/A_5'
1.4	0.49	1.4581	–0.06508	0.001356
1.2	.36	1.3431	–.047025	.00716
1.0	.25	1.242	–.03222	.00034
.75	.1406	1.138	–.01788	.00105
.5	.0625	1.062	–.00787	.00002
0	0	1	0	0

TABLE II.

kc_o	$J_1(kc_o)$	$N_1(kc_o)$	$C_{(2)}/C_{(1)}$	$J_1(kc_o)+\frac{C_{(2)}}{C_{(1)}}N_1(kc_o)$
0	0	8	0	0
.5	.2422	–1.4717	–.1022	.3926
1.0	.4400	–.7812	–.2396	.6272
1.2	.4983	–.6211	–.234	.6433
1.4	.5419	–.4791	–.1851	.6305
1.5	.558	–.4323		

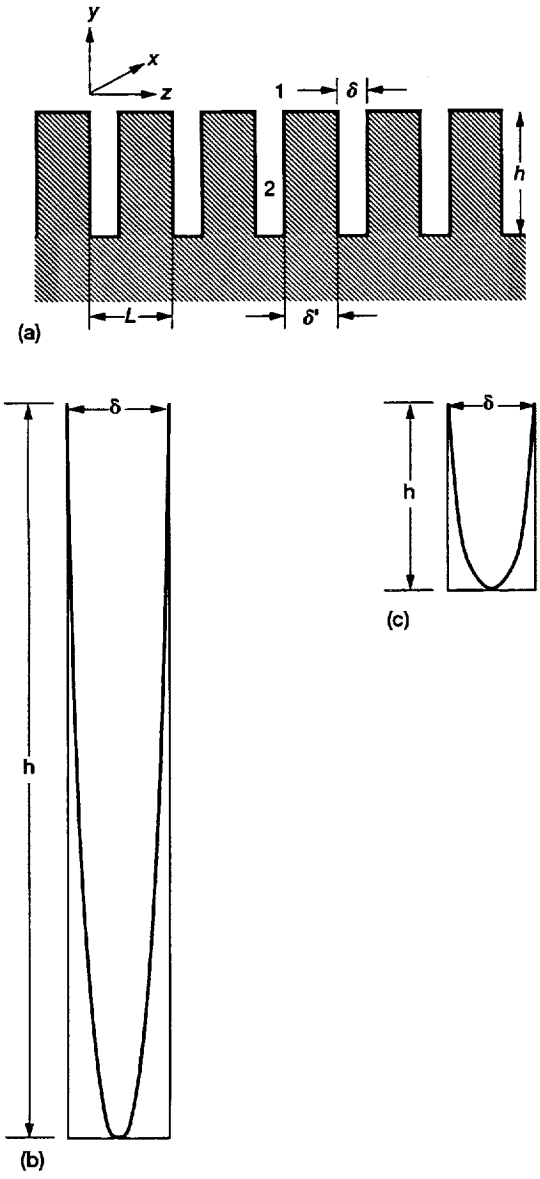

Figure 1.—(a) Cross-section of a two-dimensional vane structure with rectangular slots. Y = 0 at top of vanes and slots. Rectangular and elliptical slots, relative sizes. (b) High power fundamental circuit. (c) T-Hz BWO harmonic circuit.

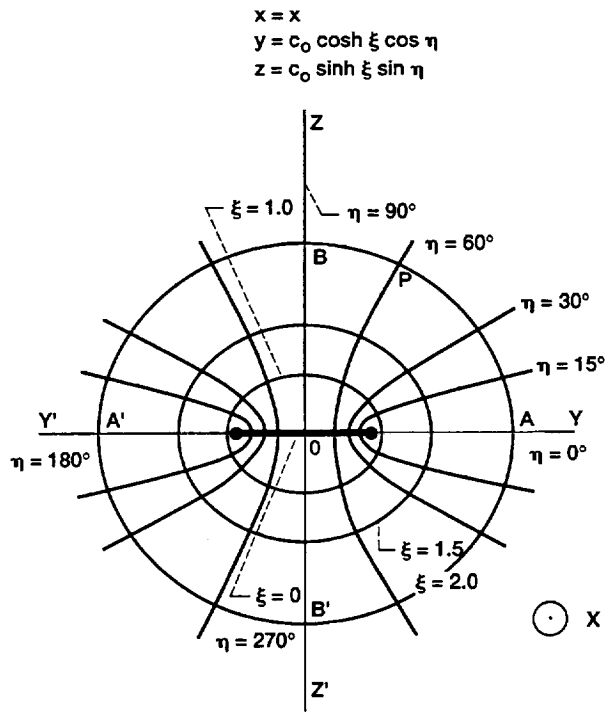

Figure 2.—Ellipses and hyperbolas with elliptical coordinates ξ and η.

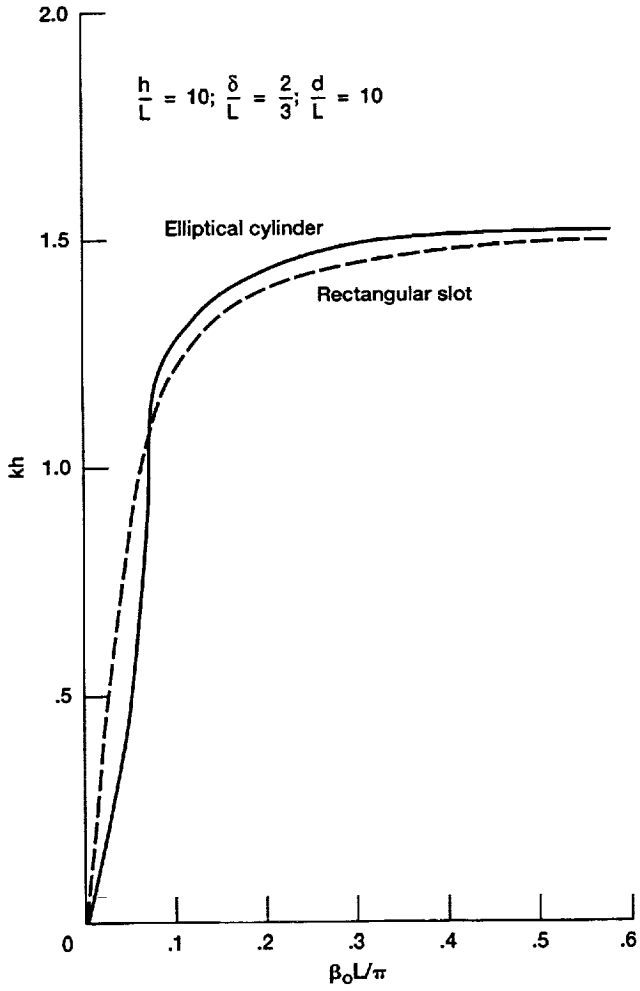

Figure 3.—Dispersion relation kh versus B_0L/π for rectangular and elliptical cross-section slots.

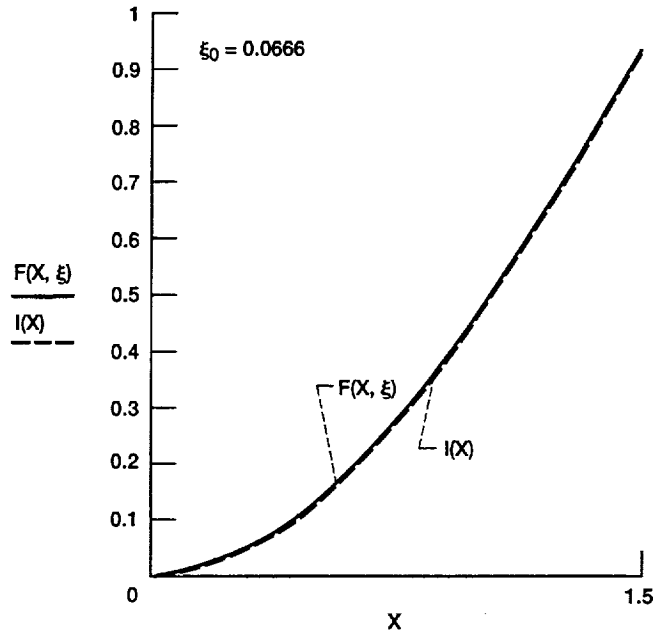

Figure 4a.—$F(x_1\xi_0)$ and I(x) versus x = kh for $\xi_0 = 0.0666$.

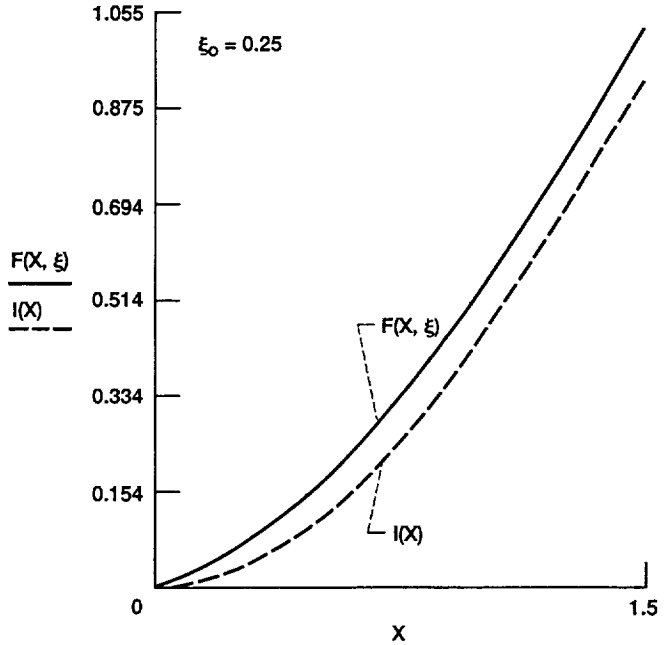

Figure 4b.—$F(x_1\xi_0)$ and I(x) versus x = kh for $\xi_o = 0.25$ (BWO case).

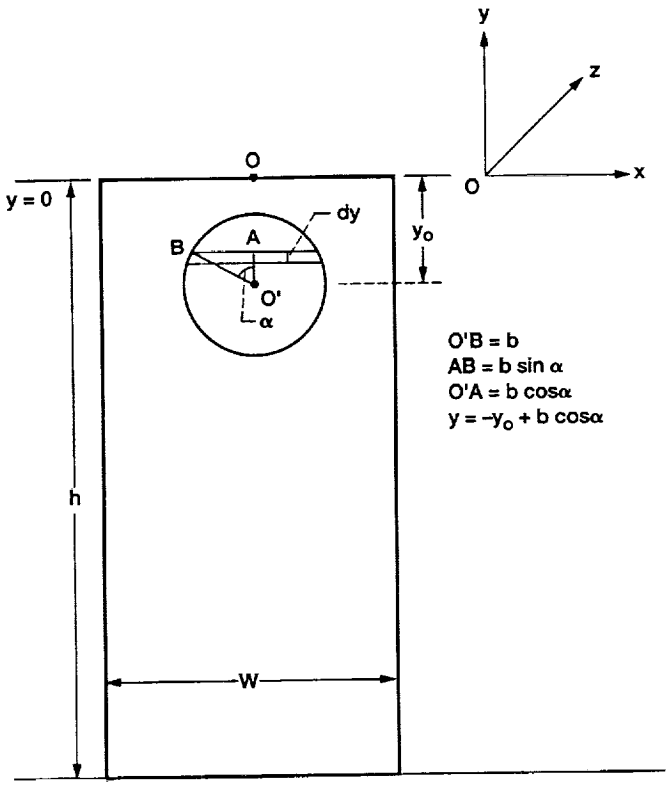

Figure 5.—Evaluation of the transverse beam coupling coefficient. The O of the coordinate system is located at the center top of the vane.

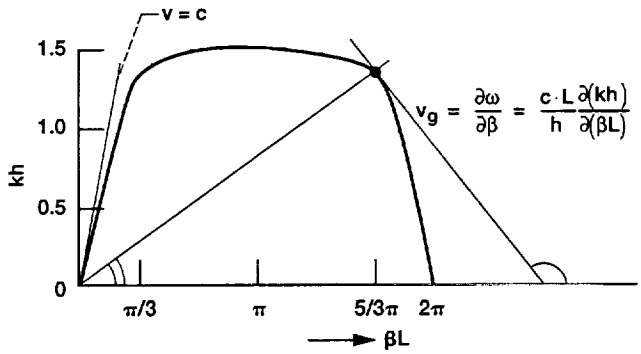

Figure 6.—Operational point for the BW harmonic.

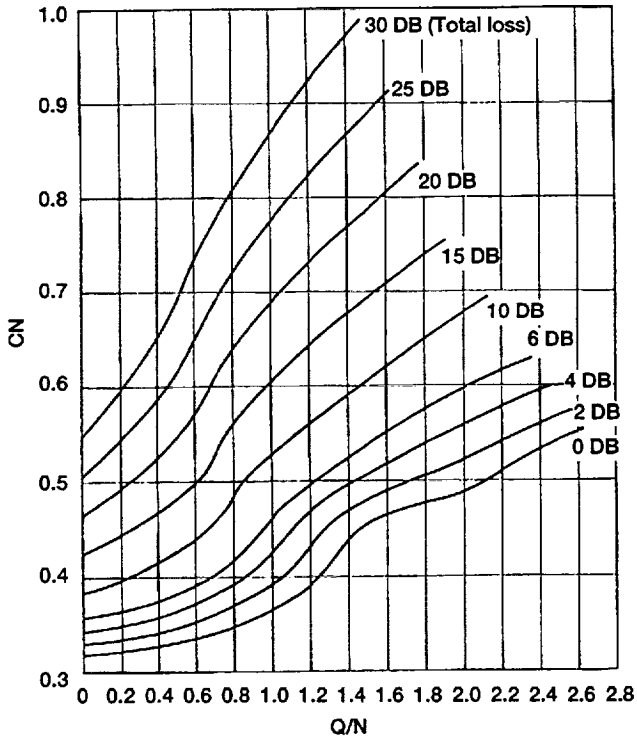

Figure 7.—Oscillations are produced in a backward-wave oscillator for values of CN equal to or greater than the value give above. Its value is a function of the space-charge parameter and the total circuit loss. From Proc IRE.

REPORT DOCUMENTATION PAGE

Form Approved
OMB No. 0704-0188

1. AGENCY USE ONLY (Leave blank)	2. REPORT DATE	3. REPORT TYPE AND DATES COVERED
	November 1994	Final Contractor Report

4. TITLE AND SUBTITLE

Slow Wave Vane Structure With Elliptical Cross-Section Slots, an Analysis

5. FUNDING NUMBERS

WU–235–01–0A
C–NAS3–25776

6. AUTHOR(S)

Henry G. Kosmahl

7. PERFORMING ORGANIZATION NAME(S) AND ADDRESS(ES)

Analex Corporation
3001 Aerospace Parkway
Brook Park, Ohio 44142

8. PERFORMING ORGANIZATION REPORT NUMBER

E–8888

9. SPONSORING/MONITORING AGENCY NAME(S) AND ADDRESS(ES)

National Aeronautics and Space Administration
Lewis Research Center
Cleveland, Ohio 44135–3191

10. SPONSORING/MONITORING AGENCY REPORT NUMBER

NASA CR–195352

11. SUPPLEMENTARY NOTES

Project Manager, James A. Dayton, Space Electronics Division, NASA Lewis Research Center, organization code 5620, (216) 433–3515.

12a. DISTRIBUTION/AVAILABILITY STATEMENT

Unclassified - Unlimited
Subject Categories 32 and 33

12b. DISTRIBUTION CODE

13. ABSTRACT ***(Maximum 200 words)***

Mathematical analysis of the wave equation in cylinders with elliptical cross-section slots was performed. Compared to slow wave structures with rectangular slots higher impedance and lower power dissipation losses are evident. These features could lead to improved designs of traveling wave magnetrons and gigahertz backward-wave oscillators as well as linear traveling wave tubes with relatively shallow slots.

14. SUBJECT TERMS

Elliptical slots; Slow wave vane structure

15. NUMBER OF PAGES

32

16. PRICE CODE

A03

17. SECURITY CLASSIFICATION OF REPORT	18. SECURITY CLASSIFICATION OF THIS PAGE	19. SECURITY CLASSIFICATION OF ABSTRACT	20. LIMITATION OF ABSTRACT
Unclassified	Unclassified	Unclassified	

National Aeronautics and
Space Administration

Lewis Research Center
21000 Brookpark Rd.
Cleveland, OH 44135-3191

DOC #: 33864 ABSTRACT SCREEN PAGE: 1 ** WORDS NOT FOUND *

Slow wave vane structure with elliptical cross-sec
tion slots, an analysis

ABQ: NC
ABA: Author

CIN: SAF
KIN: JXP
AIN:

Mathematical analysis of the wave equation in cylinders with elliptical cross-section slots was performed. Compared to slow wave structures with rectangular slots higher impedance and lower power dissipation losses are evident. These features could lead to improved designs of traveling wave magnetrons and gigahertz backward-wave oscillators as well as linear traveling wave tubes with relatively shallow slots.

PF1=ABA LIST; PF2=RESET; PF3=SIGNON; PF4=RELEASE FROM SUBQ; PF5=SELECTION;
PF6=SUBQUEUE; PF7=STORE ABSTRACT; PF8=MAI; PF10=SEND TO 'MAIQ';
PF14=PREVIOUS PAGE; PF15=NEXT PAGE; PF19=TITLE-EXT; PF20=INDEX TERMS
4B• A =-•PC LINE 11 COL 2

DOC NUMBER: 33864 INDEXING: SUBJECT/TERMS SCREEN CIN: SAF
TITLE: Slow wave vane structure with elliptical cross-sec KIN: JXP
tion slots, an analysis AIN:

	MAJOR TERMS:	SWITCH
1:	VANES	_
2:	SLOTS	_
3:	WAVE EQUATIONS	_
4:	MAGNETRONS	_
5:	BACKWARD WAVES	_
6:	MICROWAVE OSCILLATORS	_
7:	TRAVELING WAVE TUBES	_
8:	CYLINDRICAL BODIES	_
9:	MATHEMATICAL MODELS	_
10:	COUPLING COEFFICIENTS	_
11:		_
12:		_
13:		_
14:		_
15:		_

	MINOR TERMS:	
1:	IMPEDANCE	_
2:	HARMONICS	_
3:	ELECTRON BEAMS	_
4:		_
5:		_
6:		_
7:		_
8:		_
9:		_
10:		_
11:		_
12:		_
13:		_
14:		_
15:		_

PROPOSED TERMS:

PF2=RESET; PF3=SIGNON; PF4=RELEASE; PF5=SELECTION; PF6=SUBQ
PF10=ALPHA; PF11=HIERARCHY; PF12=STORE; PF13=CENTRAL SCREEN; PF20=TITLE/WNF
4B• A =-•PC LINE 6 COL 11